

Effect of supporting layer on growth of carbon nanotubes by thermal chemical vapor deposition

Yunyu Wang,^{a)} Bin Li, and Paul S. Ho

Microelectronics Research Center, The University of Texas at Austin, Austin, Texas 78712

Zhen Yao

Department of Physics, The University of Texas at Austin, Austin, Texas 78712

Li Shi

Department of Mechanical Engineering, The University of Texas at Austin, Austin, Texas 78712

(Received 2 May 2006; accepted 19 September 2006; published online 2 November 2006)

Selective growth of vertically aligned and highly dense carbon nanotubes was achieved by using thermal chemical vapor deposition via careful selection of a thin catalyst layer and an appropriate supporting layer. It was found that carbon nanotube growth was significantly enhanced when tantalum was used as the supporting layer on which a thin iron catalyst was deposited. Cross-sectional transmission electron microscopy revealed a Stranski-Krastanov mode of iron island growth on tantalum with relatively small contact angles controlled by the relative surface energies of the supporting layer, the catalyst, and their interface. The as-formed iron island morphology promoted vertical growth of carbon nanotubes. © 2006 American Institute of Physics.

[DOI: [10.1063/1.2382735](https://doi.org/10.1063/1.2382735)]

Carbon nanotubes (CNTs) have shown remarkable current carrying capability, thermal conductivity, and mechanical strength.^{1–3} These superior properties have generated great interest for applications in ultralarge scale integrated circuits (ULSIs),^{4–6} field emission displays,^{7,8} thermal interface materials,⁹ and others. These applications often require uniform, oriented, and high-density CNTs selectively grown on patterned electrodes. It has been demonstrated that CNT growth can be controlled using appropriate catalyst particles or film thickness,^{10,11} precursors,¹² temperatures, pressures,¹³ and applied electrical field.¹⁴ Here we report the selective growth of vertically aligned and highly dense CNT arrays using a simple thermal catalytic chemical vapor deposition (CCVD) method via careful selection of the supporting layer on which the thin catalyst layer is deposited. It was found that the supporting layer can tune the shapes and curvatures of the catalyst particles, which are controlled by the relative surface energies of the supporting layer, the catalyst, and their interface. Cross-sectional transmission electron microscopy (TEM) revealed a Stranski-Krastanov mode of iron (Fe) island growth on tantalum (Ta), with relatively small contact angles of the islands. The as-formed Fe island morphology promoted vertical growth of the CNTs from the catalyst surface. This finding suggests a different and simple route to control growth of oriented CNT arrays, and is a step toward the use of CNTs for various applications.

CNTs were grown using thermal CCVD. Fe thin films with thicknesses of 3–9 nm were deposited by electron beam evaporation and used as catalyst. CNT growth was conducted in a quartz tube furnace. During the growth, the furnace was ramped up from room temperature to 700 °C in hydrogen (H₂) with a flow rate of 1 l/min, and stabilized at 700 °C for 1 min; then the growth was initiated by introducing acetylene (C₂H₂) into the furnace with a flow rate of 100 ml/min. The growth was conducted at atmospheric pres-

sure and the growth time varied from 1 to 6 min.

The CNTs were grown from a bilayer template consisting of a thin layer of metal catalyst on a supporting layer. A proper combination of the catalyst and the supporting layer material can lead to uniform and dense catalyst islands for seeding CNT growth. In our early experiments, CNTs were directly grown using the CCVD method on SiO₂ substrates, and most of the CNTs were found to be randomly distributed and tangled yielding a low density and poor film coverage. Subsequently, we conducted the CCVD growth of CNTs on prepatterned wafers consisting of copper interconnect structures covered by a tantalum barrier layer and observed the growth of vertically aligned CNTs. The Fe/Ta bilayer appeared to provide a proper template for selective growth of vertically aligned and dense CNT films. This surprise finding has motivated us to carry out this study to investigate different supporting materials.

Fe catalysts with the same thicknesses of about 3 nm were deposited on different substrates including 300 nm thick SiO₂ film as well as 20 nm thick Ta, palladium (Pd), and chromium (Cr) layers on SiO₂. We found that Fe on Cr and Fe on SiO₂ produced randomly aligned CNTs with low-density film coverage, whereas Fe on Pd resulted in the lowest growth yield, as shown in Figs. 1(a)–1(c). Only in the case of Fe on Ta, the growth was greatly enhanced yielding CNTs with high density and uniformity, as shown in Fig. 1(d). Moreover, we found that vertically aligned dense CNTs were always obtained within a range of Fe film thicknesses from 3 to 9 nm on the Ta support. In this thickness range, the densities of CNT films were found to decrease with increasing Fe thickness. On the contrary, random growth with poor coverage was always observed on the SiO₂, Cr, and Pd substrates irrespective of the Fe film thickness. These results were reproducible in five experiments of different thicknesses with the Cr and Pt supports, and in ten experiments for Ta and SiO₂ supports. Additionally, we have investigated different supporting layer thicknesses ranging from

^{a)}Electronic mail: yywang@mail.utexas.edu

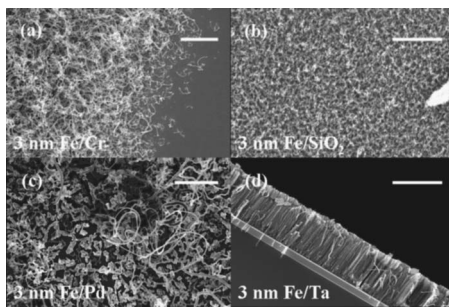


FIG. 1. SEM images of CNTs grown on different supporting materials. [(a)–(c)] Top-view SEM images of CNTs grown with 3 nm thick Fe deposited on Cr, Pd, and SiO₂, respectively (scale bars: 2 μm). (d) Cross-sectional SEM image of CNTs grown on 3 nm thick Fe deposited on Ta (scale bar: 8 μm).

5 to 50 nm and found no apparent effects on the CNT growth. CNTs obtained from Ta and SiO₂ have also been characterized by high resolution TEM. It was found that CNTs are multiwalled with diameters of 5–20 nm. Fe particles were found at the bottom of CNTs on Ta and the tips of CNTs on SiO₂, which suggests that the base growth mode and tip growth mode are applied on Ta and SiO₂, respectively.

To investigate how the supporting materials affect the formation of the catalyst islands that are responsible for the CNT growth, we used a scanning electron microscope (SEM) to examine the Fe islands on different supporting materials after the Fe films had been annealed at 700 °C for 1 min. The surface morphologies were shown in Figs. 2(a)–2(d). For a 3 nm thick Fe layer deposited on Ta, the Fe islands showed a narrow range of size distribution from about 13 to 30 nm, and the Fe islands were densely packed reaching a density of about $1.6 \times 10^{11}/\text{cm}^2$, as shown in Fig. 2(a). Similarly, the Fe islands formed on SiO₂ were about 10–35 nm in size with a density about $1.3 \times 10^{11}/\text{cm}^2$ [Fig. 2(b)]. Figures 2(c) and 2(d) show the morphologies of 3 nm thick Fe layers deposited on the Cr layer and the Pd layer, respectively. The Fe layer on Cr was found to be continuous with a very rough surface, and the Fe layer on Pd exhibited isolated islands larger than 200 nm. Similar results were also observed for 9 nm thick Fe deposited on Ta, Cr, Pd, and SiO₂ and annealed under the same condition.

We have also annealed the different supporting layers without the Fe catalyst under the same condition. The Ta

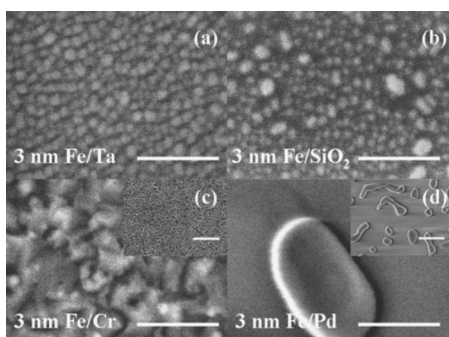


FIG. 2. SEM images of surface morphologies of annealed Fe layer on Ta, SiO₂, Cr, and Pd. Initial Fe film thickness is 3 nm. Insets to (c) and (d) are SEM images of the surfaces of the Cr and Pd supporting layers after annealing without Fe deposition. Scale bars are 200 nm for [(a)–(d)] and 1 μm for all insets.

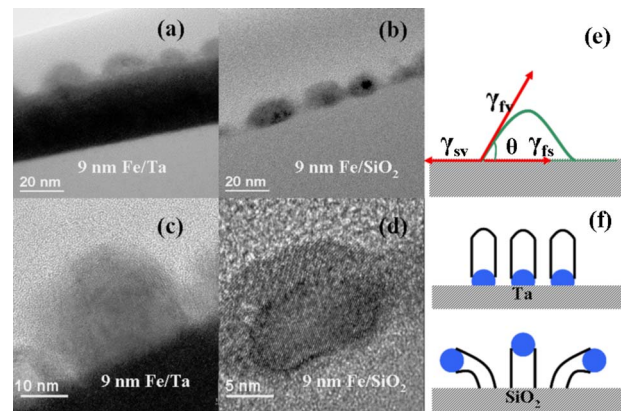


FIG. 3. (Color online) Low resolution cross-sectional TEM images of Fe islands formed on (a) Ta and (b) SiO₂. High resolution cross-sectional TEM images of Fe islands on (c) Ta and (d) SiO₂. (e) Schematic of the catalyst island formation under the balance of the surface energies. (f) Schematics of CNT growth on the Fe catalyst particles, where CNTs grow vertically on the catalysts on the Ta support and randomly on the catalysts on SiO₂.

support was found to exhibit a smooth surface without pinholes after annealing, which we believe is responsible for the formation of fine uniform Fe islands. On the other hand, both the Cr and Pd films became discontinuous with pinholes and large islands, as shown in the insets of Figs. 2(c) and 2(d). These films are thus not favorable for the formation of small and uniform Fe islands.

Although Fe island size and distribution are similar in the case of Ta and SiO₂ supports, distinctly different growth scenarios were observed. In order to gain further insights, cross-sectional TEM was used to investigate the morphologies of the annealed Fe islands on the Ta and SiO₂ substrates. Figs. 3(a)–3(d) are typical TEM images of Fe islands formed after a 9 nm thick Fe layer was deposited and annealed on Ta and SiO₂. For each supporting layer, about 50 Fe particles were examined. The island shape was distinctly different. On the Ta substrate, they had a hemispherical shape and relatively small contact angles ranging between 40° and 90°. On the SiO₂ substrate, on the other hand, they exhibited a bead shape with much larger contact angles of 130°–180°.

Previously, efforts have been made to optimize CNT growth process by adding a supporting layer below the catalyst layer or using a metal multilayer or mixture to prevent the catalyst from reacting with or diffusing into the substrates, to enhance catalyst activities, or to improve the adhesion between the catalyst layer and the substrate.^{4,15–23} Our present study shows that the supporting layer can also be used to tune the shapes and curvatures of the catalyst particles.²⁴ The morphology and contact angle of the Fe islands can be accounted for by considering the balance of the surface energies for the islands, as shown in Fig. 3(e),

$$\cos \theta = (\gamma_{sv} - \gamma_{fs}) / \gamma_{fv}, \quad (1)$$

where θ is the contact angle, and f , s , and v represent the film, substrate, and vacuum, respectively, and a pair of the subscripts refers to the interface between the indicated phases. In the case of Fe on Ta, $0 < \cos \theta < 1$, implying that the surface energy of the Ta substrate exceeds that of the Fe/Ta interface. In contrast, for the Fe island on SiO₂, $-1 < \cos \theta < 0$, implying that the surface energy of SiO₂ is less than that of the Fe/SiO₂ interface. Although the energies of these particular interfaces have not been measured, the ob-

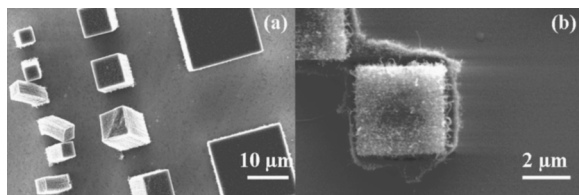


FIG. 4. SEM images of patterned vertically aligned CNTs with high densities. (a) 5, 10, and 20 μm wide CNT columns grown on predefined patterns consisting of 3 nm thick Fe on the Ta support. (b) 4 μm wide CNT films grown in via holes, on the bottom of which 3 nm thick Fe was deposited on Ta.

served morphologies of the Fe islands are consistent with the relative magnitudes of the reported surface energies, i.e., $\sim 2100\text{--}2200$ ergs/cm² for Ta,²⁵ 43–106 ergs/cm² for SiO₂,²⁶ and 1880–2150 ergs/cm² for Fe.²⁷ These surface and interface energies also control the island sizes formed on the substrate depending on the amount of Fe overlayer deposited.

The curvatures and shapes of catalyst particles are essential for the growth of CNTs.²⁸ They can greatly affect where the nucleation of CNTs occurs at the catalyst surface, and lead to distinctly different growth scenarios: oriented versus random. We believe that at the beginning the growth of CNTs along the vertical direction is facilitated by an acute θ as in the case of Fe on Ta, but not for an oblique θ as in the case of Fe on SiO₂ [Fig. 3(f)]. Combined with the formation of uniform and dense Fe islands with a narrow size distribution on the Ta support, dense CNTs can support each other to grow in the vertical direction.

To demonstrate the versatility of our approach, we have used electron beam lithography (EBL) and a lift-off process to form 5, 10, and 20 μm wide square patterns of 3 nm thick Fe on 20 nm thick Ta support, and used the thermal CCVD method to grow aligned CNT columns on the patterns, as shown in Fig. 4(a). We have also employed the method using a Ta support to grow CNT films in patterned via holes. In the fabrication process, a 20 nm thick Ta layer was sputtered on the substrate and a 500 nm thick SiO₂ film was deposited on the Ta layer. About 260 nm thick polymethyl-methacrylate (PMMA) was spun on the SiO₂ film and patterned using EBL. Via holes were etched into the SiO₂ film with the PMMA pattern as an etching mask. Subsequently, a 3 nm thick Fe layer was deposited on the wafer. Only the Fe and Ta films deposited on the bottom of the via holes were left after the PMMA layer was stripped in acetone. As shown in Fig. 4(b), highly dense CNTs were grown from the Fe catalyst patterned at the bottom of the 4 μm wide via hole. Our method can be readily used to grow CNT via structures on ULSI copper interconnect structures since Ta is used as the barrier layer on copper interconnects. This method can also be used for the selective growth of highly dense, vertically

aligned, and high-quality CNTs directly on a metal electrode for other applications.

The authors are grateful for the support from SEMATECH through Advanced Materials Research Center (AMRC), the fabrication and characterization facilities in Microelectronic Research Center (MER), and the Center of Nano and Molecular Science and Technology (CNM) at the University of Texas at Austin. The authors thank Xiaoxia Gao and Jiping Zhou for assistance on TEM and Zhiqian Luo for mapping island distribution.

- ¹Z. Yao, C. L. Kane, and C. Dekker, *Phys. Rev. Lett.* **84**, 2941 (2000).
- ²P. Kim, L. Shi, A. Majumdar, and P. L. McEuen, *Phys. Rev. Lett.* **87**, 215502 (2001).
- ³E. W. Wong, P. E. Sheehan, and C. M. Lieber, *Science* **277**, 1971 (1997).
- ⁴M. Horibe, M. Nihei, D. Kondo, A. Kawabata, and Y. Awano, *Jpn. J. Appl. Phys., Part 1* **44**, 5309 (2005).
- ⁵P. Avouris, *Chem. Phys.* **281**, 429 (2002).
- ⁶P. L. McEuen, M. Fuhrer, and H. Park, *IEEE Trans. Nanotechnol.* **1**, 78 (2002).
- ⁷W. A. de Heer, A. Châtelain, and D. Ugarte, *Science* **270**, 1179 (1995).
- ⁸Q. H. Wang, A. A. Setlur, J. M. Lauerhaas, J. Y. Dai, E. W. Seelig, and R. P. H. Chang, *Appl. Phys. Lett.* **72**, 2912 (1998).
- ⁹P. Schelling, L. Shi, and K. E. Goodson, *Mater. Today* **8**, 30 (2005).
- ¹⁰Y. Y. Wang, S. Gupta, R. J. Nemanich, Z. J. Liu, and C. Q. Lu, *J. Appl. Phys.* **98**, 014312 (2005).
- ¹¹S. Hofmann, M. Cantoro, B. Kleinsorge, C. Casiraghi, A. Parvez, J. Robertson, and C. Ducati, *J. Appl. Phys.* **98**, 034308 (2005).
- ¹²G. Eres, A. A. Puzos, D. B. Geohegan, and H. Cui, *Appl. Phys. Lett.* **84**, 1759 (2004).
- ¹³H. Cui, O. Zhou, and B. R. Stoner, *J. Appl. Phys.* **88**, 6072 (2000).
- ¹⁴Y. Zhang, A. Chang, J. Cao, Q. Wang, W. Kim, Y. Li, N. Morris, E. Yenilmez, J. Kong, and H. Dai, *Appl. Phys. Lett.* **79**, 3155 (2001).
- ¹⁵S. Fan, M. G. Chapline, N. R. Franklin, T. W. Tombler, A. M. Cassell, and H. Dai, *Science* **283**, 512 (1999).
- ¹⁶Z. J. Zhang, B. Q. Wei, G. Ramanath, and P. M. Ajayan, *Appl. Phys. Lett.* **77**, 3764 (2000).
- ¹⁷L. Delzeit, C. V. Nguyen, B. Chen, R. Stevens, A. Cassell, J. Han, and M. Meyyappan, *J. Phys. Chem. B* **106**, 5629 (2002); H. T. Ng, B. Chen, J. E. Koehne, A. M. Cassell, J. Li, J. Han, and M. Meyyappan, *ibid.* **107**, 8484 (2003).
- ¹⁸H. Hongo, F. Nihey, T. Ichihashi, Y. Ochiai, M. Yudasak, and S. Ijima, *Chem. Phys. Lett.* **380**, 158 (2003).
- ¹⁹J. I. Sohn, C. Nam, and S. Lee, *Appl. Surf. Sci.* **197–198**, 568 (2002).
- ²⁰A. M. Cassell, Q. Ye, B. A. Cruden, J. Li, P. C. Sarrazin, H. T. Ng, J. Han, and M. Meyyappan, *Nanotechnology* **15**, 9 (2004).
- ²¹K. M. Lee, H. J. Han, S. Choi, K. H. Park, S. Oh, S. Lee, and K. H. Koh, *J. Vac. Sci. Technol. B* **21**, 623 (2003).
- ²²M. Cantoro, S. Hofmann, S. Pisana, V. Scardaci, A. Parvez, C. Ducati, A. C. Ferrari, A. M. Blackburn, K. Wang, and J. Robertson, *Nano Lett.* **6**, 1107 (2006).
- ²³D. E. Resasco, W. E. Alvarez, F. Pompeo, L. Balzano, J. E. Herrera, B. Kitiyanan, and A. Borgna, *J. Nanopart. Res.* **4**, 131 (2002).
- ²⁴A. L. Giermann, and C. V. Thompson, *Appl. Phys. Lett.* **86**, 121903 (2005).
- ²⁵P. Paradis, T. Ishikawa, and S. Yoda, *J. Appl. Phys.* **97**, 053506 (2005).
- ²⁶C. Sun and J. C. Berg, *J. Chromatogr., A* **969**, 59 (2002).
- ²⁷G. A. Somorjai, *Chemistry in Two Dimensions: Surfaces* (Cornell University Press, Ithaca, 1981), p. 31.
- ²⁸S. Helveg, C. López-Cartes, J. Sehested, P. L. Hansen, B. S. Clausen, J. R. Rostrup-Nielsen, F. Abild-Pedersen, and J. K. Nørskov, *Nature (London)* **427**, 426 (2004).